Laser Phase Relations of High-Order Harmonic Generation

GE Yu-Cheng(葛愉成)*

Department of Technical Physics, Peking University, Beijing 100871

(Received 15 May 2006)

Laser phase relations of high-order harmonic generation (HHG) are calculated with the saddle point theory. The results show a two-peak structure including a symmetric and an asymmetric temporal distributions of the instantaneous frequency of HHG radiation. These distributions are fitted with Gaussian and polynomial functions, respectively. Two calculation formulae are presented to analyse attosecond x-rays with specified time duration and energy bandwidth in experiments.

PACS: 42. 65. Re, 42. 65. Ky, 32. 80. Rm, 42. 30. Rx

Ultra-fast measurements need increasingly shorter x-ray pulses. Usually, we know what happens in a chemical or bio-chemical reaction. However, it is difficult to realize how a reaction occurs. Still, knowing how a reaction occurs is essential for further research and control of the reaction. The dynamic process of a chemical or biochemical reaction involves energy and electron transfers that typically occur on femto- and sub-femtosecond time scales. Today, studying and measuring such a dynamic process is one of the scientific frontiers, which attracts much attention. However, in order to know the reaction dynamic processes, temporally much shorter extreme ultraviolet (EUV) or x-ray pules are necessary. Particularly, x-rays in a water window have their own advantages in bio-chemical research. The energy of x-ray in water window ranges between the K absorption edges of carbon (283.7 eV) and oxygen (532.1 eV), where carbon-containing biological objects absorb radiation efficiently while water (oxygen and hydrogen) is comparatively transparent.

Both theoretical and experimental research makes it interesting to study laser-phase-dependent high-order harmonic generation (HHG). In 1994, Lewenstein *et al.*[1] presented their quantum theory to describe the HHG radiation of an atom in a strong laser field. So far, HHG has been a successful way to produce EUV and x-rays in water window.[2,3] Recently, researchers[4−6] have reported successful generation of 650-as (1 as= 10^{-18} s) isolated EUV pulses. In measurement, I reported transfer equations and the related laser phase determination methods.[7−9] With these equations and methods, detailed intensity temporal structures and instantaneous frequency of fs and as x-ray pulses can be directly reconstructed from the measured photoelectron spectra, including not only the time duration of a single pulse but also the asymmetry and side-band structures of the pulse.

Further study of the laser-phase-dependent HHG radiation may improve the attosecond x-ray sources and the separation of the single x-ray pulse. According to the cut-off law,[1] the highest energy of HHG radiation is about $\hbar\omega_X = 1.32I_p + 3.17U_p$, where ω_X is the angular frequency of the HHG radiation, I_p is the atomic ionization potential, and U_p is the ponderomotive energy of the electron in a strong laser field. In order to produce x-rays in water window, it is necessary to increase the intensity of a few-cycle laser to the order of $10^{15}\,\mathrm{W/cm^2}$. With the development of state-of-the-art ultrashort laser systems,[1,10,11] it is easy to reach such intensities. Therefore, it is possible to optimize the attosecond x-ray sources to generate reproducible pulses with specified durations and energy bandwidths for applications. In this Letter, we calculate interesting HHG laser phase relations using Lewenstein's saddle point theory.[1]

Our exploration begins with the time-dependent Shrödinger equation

$$i\frac{\partial}{\partial t}|\Psi(\boldsymbol{r},t)\rangle = \Big[-\frac{1}{2}\nabla^2 + V(\boldsymbol{r}) - E\cos(t)x\Big]|\Psi(\boldsymbol{r},t)\rangle, \tag{1}$$

where $|\Psi(\boldsymbol{r},t)\rangle$ is an electron wave function in a single-electron approximation under the influence of a laser field $E\cos t$. The laser is linearly polarized in the x direction, and $V(\boldsymbol{r})$ is the atomic potential. For simplicity, we use atomic units, but express all energies in terms of the laser photon energy. Initially, the system is in the ground state, denoted as $|0\rangle$, which in general has a spherical symmetry.

We take the following assumptions for the regime of parameters we consider.[1] (a) The contribution to the evolution of the system of all bound states except the ground state $|0\rangle$ can be neglected. (b) The depletion of the ground state can be neglected ($U_p < U_{\mathrm{sat}}$, here U_{sat} is the saturation level of U_p when all atoms ionize during the interaction time). (c) In the continuum, the electron can be treated as a free particle moving in the laser field with no effect of $V(\boldsymbol{r})$. If we neglect the contribution from the continuum-continuum part, i.e. we consider only the transition back to the ground state, then the x component of the

* Email: gzgyc@sina.com

©2006 Chinese Physical Society and IOP Publishing Ltd

time-dependent dipole moment, $x(t) = \langle\Psi(t)|x|\Psi(t)\rangle$, can be expressed by an integral over the canonical momentum, $\boldsymbol{p}$

$$x(t) = i\int_0^t dt' \int d^3\boldsymbol{p} E\cos(t') d_x(\boldsymbol{p} - \boldsymbol{A}(t')) \cdot d_x^*(\boldsymbol{p} - \boldsymbol{A}(t)) e^{-iS(\boldsymbol{p},t,t')} + \text{c.c.}, \quad (2)$$

where $\boldsymbol{A}(t) = (E\sin(t), 0, 0)$ is the vector potential of the laser field; $\boldsymbol{d}(\boldsymbol{p}) = \langle\boldsymbol{p}|\boldsymbol{r}|0\rangle$ denotes the atomic dipole matrix element for the bound-free transition; and $d_x(\boldsymbol{p})$ is the component parallel to the polarization axis. The quasi-classical action reads

$$S(\boldsymbol{p}, t, t') = \int_{t'}^t dt'' \Big\{\frac{[\boldsymbol{p} - \boldsymbol{A}(t'')]}{2} + I_p\Big\}. \quad (3)$$

The spectrum or the amplitude of $(2K+1)$-th harmonic radiation is given by the Fourier transform of $x(t)$,

$$x_{2K+1} = \frac{1}{2\pi}\int_{t_0}^{t_0+2\pi} dt x(t) e^{(2K+1)it}. \quad (4)$$

According to Lewenstein's theory,[1] the dominant contribution to the harmonic emission comes from the electrons which tunnel away from the nucleus at time t' then reencounter it at t while oscillating in the laser field. The saddle-point equations that arise from the derivatives of the quasi-classical action of Eq. (3) take the forms

$$\nabla_p S(\boldsymbol{p}, t, \tau) = \boldsymbol{r}(t) - \boldsymbol{r}(t-\tau) = 0, \quad (5)$$

$$\frac{\partial S(\boldsymbol{p}, t, \tau)}{\partial \tau} = \frac{[\boldsymbol{p} - \boldsymbol{A}(t-\tau)]^2}{2} + I_p = 0, \quad (6)$$

$$\frac{\partial S(\boldsymbol{p}, t, \tau)}{\partial t} = \frac{[\boldsymbol{p} - \boldsymbol{A}(t)]^2}{2} - \frac{[\boldsymbol{p} - \boldsymbol{A}(t-\tau)]^2}{2} = 2K + 1, \quad (7)$$

where τ is defined as the electron return time, $\tau = t - t'$. Equation (5) indicates that the only relevant electron trajectories are located at the positions where the electron leaves the nucleus at birth time $t - \tau$ and returns at recombination time t. Equation (6) has a complex resolution of τ, and its imaginary part can be interpreted as the tunnelling time. Equation (7) is simply the energy conservation law, which gives the final kinetic energy of the recombining electron that generates the $(2K+1)$th harmonic radiation.

Let us calculate the energy of radiation. In the classical view, the conserved canonical momentum due to neglecting the effects of $V(\boldsymbol{r})$ can be written as $p_{st}(t, \tau) = E[\cos t - \cos t(t-\tau)]/\tau$. The electron kinetic energy gain at time t reads

$$\Delta E_{kin}(\tau) = \frac{[p_{st}(t,\tau) - A(t)]^2}{2} - \frac{[p_{st}(t,\tau) - A(t-\tau)]^2}{2}. \quad (8)$$

The thick solid line in Fig. 1(a) presents the energy gain $\Delta E_{kin}(\tau)/U_p$ as a function of the return time τ.

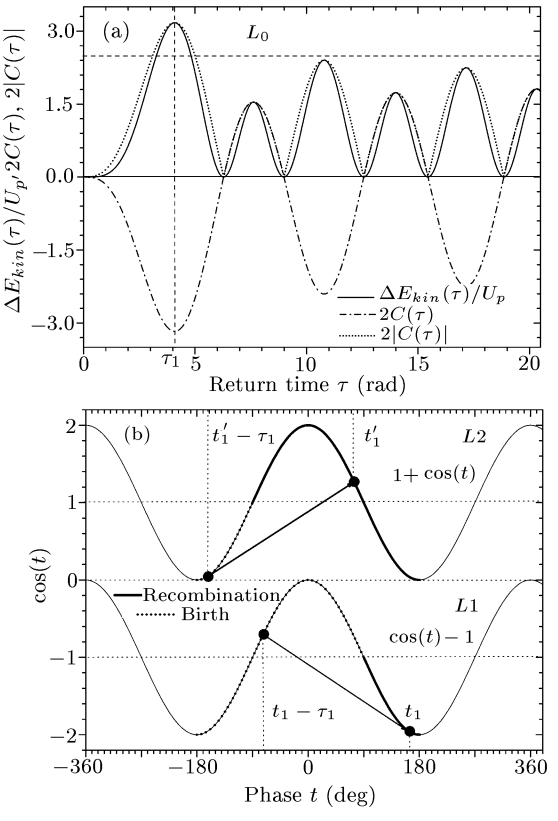


Fig. 1. (a) The kinetic energy gain $\Delta K_{kin}(\tau)/U_p$ (thick solid line) and the function $2|C(\tau)|$ (dotted curve) versus the return time τ. Note that both the functions have the same maxima at the same values of τ and that the high energy radiations for $\Delta K_{kin}(\tau)/U_p > 2.5$ occur only in the range of τ between 3.3–4.8 rad. (b) The illustration of electron birth and recombination phases of HHG in a laser optical cycle. Lines L1 and L2 present the changes of the laser electric field. The electron born at time $t - \tau$ (shown in the time range of the dotted curve) and returned to the same position at time t (shown in the time range of the thick solid curve) radiates a harmonic wave. These dotted and thick solid curve pairs correspond to the solutions to Eqs. (12) and (13), respectively. Each arrow starting from the specified birth time to the recombination time denotes the highest energy radiation.

In the quantum view, the value of the quasi-classical action of Eq. (3) is

$$S_{st}(t, \tau) = (I_p + U_p)\tau - 2U_p\frac{1 - \cos(\tau)}{\tau} - U_p C(\tau)\cos(2t - \tau), \quad (9)$$

with

$$C(\tau) = \sin(\tau) - 4\sin^2(\tau/2)/\tau. \quad (10)$$

$C(\tau)$ determines the variation of $S_{st}(t, \tau)$ as a function of τ. Figure 1(a) shows $2C(\tau)$ (dot-dashed line) and $2|C(\tau)|$ (dotted line). The two curves, classical $\Delta K_{kin}(\tau)/U_p$ and quantum $2|C(\tau)|$ are remarkably similar and both have the same maxima and zeros at

the same values of τ. Moreover, the high energy radiations for $\Delta K_{kin}(\tau)/U_p > 2.5$ occur only in the range of τ for 3.3–4.8 rad, with a peak at $\tau_1 = 4.08$ rad of the highest $\Delta K_{kin,\max}(\tau)/U_p = 3.17$. This phase range is shown by the curves above line L0 in Fig. 1(a). This means that the high energy harmonic radiations are generated by electrons returned in a laser optical cycle.

At the saddle point, Eq. (6) can be reduced to

$$\sin(t-\tau) + \frac{\cos(t) - \cos(t-\tau)}{\tau} = i\sqrt{\frac{I_p}{2U_p}}. \quad (11)$$

Equation (11) has two complex-conjugated solutions,

$$\sin\left(t - \frac{\tau}{2}\right) = \frac{i\sqrt{\frac{I_p}{2U_p}}a(\tau) + s(\tau)\sqrt{a^2(\tau) + s^2(\tau) + \frac{I_p}{2U_p}}}{s^2(\tau) + a^2(\tau)}, \quad (12)$$

$$\sin\left(t - \frac{\tau}{2}\right) = \frac{i\sqrt{\frac{I_p}{2U_p}}a(\tau) - s(\tau)\sqrt{a^2(\tau) + s^2(\tau) + \frac{I_p}{2U_p}}}{s^2(\tau) + a^2(\tau)}, \quad (13)$$

where $a(\tau) = \cos(\tau) - 2\sin(\tau/2)/\tau$, $s(\tau) = \sin(\tau/2)$.

Equations (12) and (13) are used to calculate the laser phase relations at $I_p/U_p \neq 0$. Usually, numerical calculation should be performed to obtain complex solutions of the return time τ. When $I_p \ll U_p$, Eq. (11) and its solutions can be simplified to approximate forms. For example, in order to generate harmonics at water window with Helium gas ($I_p = 24.6$ eV), we can calculate U_p according to the cut-off law. The results give ranges from $U_p = 79.3$ eV to 157.6 eV and from $I_p/U_p = 0.31$ to 0.16. We write the return time $\tau = \tau_0 + i\delta$, here τ_0 is the real part, and $i\delta$ is the imaginary part that may be a small value if $I_p \ll U_p$. Expending all the terms in the left-hand side of Eq. (11) to the first order in $i\delta$, we obtain the approximation equations in which the real and imaginary parts of the return time satisfy

$$\sin(t-\tau_0) + \frac{\cos(t) - \cos(t-\tau_0)}{\tau_0} = 0, \quad (14)$$

and

$$\delta = -\frac{1}{\cos(t-\tau_0)}\sqrt{\frac{I_p}{2U_p}}. \quad (15)$$

We can find that Eq. (14) has the same form as Eq. (11) at $I_p/U_p = 0$. Regarding only to the real part of the return time, we can use the solutions of Eqs. (12) and (13) at $I_p/U_p = 0$ to calculate the laser phase relations of HHG radiation at $I_p/U_p \neq 0$.

Figure 1(b) illustrates the electron birth and return phases of HHG in a laser optical cycle. Lines L1 and L2 depict the change of the laser electric field. The electron born at time $t - \tau$ (dotted curves) and returned to the same position at time t (thick solid curves) radiates a harmonic wave. These dotted and thick solid curve pairs correspond to the solutions of Eq. (12) and (13), respectively. For $\tau_1 = 4.08$ rad (233.76°), each arrow starting from the specified birth time $t_1 - \tau_1$ (or $t_1' - \tau_1$) and ending at the recombination time t_1 (or t_1') denotes the highest energy radiation.

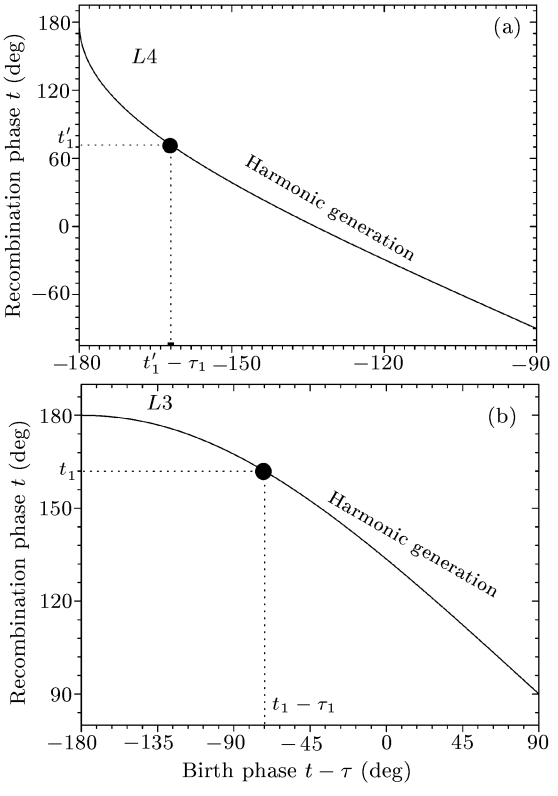


Fig. 2. Lines L4 (a) and L3 (b) are the HHG laser phase relations corresponding to the solutions of Eq. (12) and (13), respectively. Within a laser optical cycle, the electron born at the laser phase $t_1 - \tau_1 = -71.80°$ (−161.96°) and returned at $t_1 = 161.96°$ (71.80°) produces the highest energy radiation of $1.32I_p + 3.17U_p$.

The physics of HHG radiation can be directly shown as the laser phase relations in Fig. 2. These relations are the possible tracks of HHG radiation in the laser phase domain (in units of degree). Within a laser optical cycle, the electron born at the laser phase $t_1 - \tau_1 = -71.80°$ (−161.96°) and returned at $t_1 = 161.96°$ (71.80°) produces the highest energy radiation of $1.32I_p + 3.17U_p$.

Figure 3(a) shows the energy gain distribution $H_1(t)$ and $H_2(t)$ of HHG radiation versus the recombination phase t (rad) in a laser optical cycle. Here $H_{1,2}(t) = \Delta K_{kin}(\tau)/U_p$. They correspond to the solutions of Eqs. (12) and (13), respectively. The dotted line, $h_1(t) = 61.37 - 188.26t + 223.83t^2 -$

$129.14t^3 + 36.11t^4 - 3.09t^5$, is a polynomial fit of $H_1(t)$, and the dot-dot-dashed line, $h_2(t) = -0.08 + 3.29e^{-0.75(t-1.22)^2}$, is a Gaussian fit of $H_2(t)$. Obviously, $H_1(t)$ has an asymmetric shape peaked at 2.83 rad (161.96°). $H_2(t)$ has a symmetric Gaussian shape centred at 1.25 rad (71.8°). For harmonics near cut-off edge, the study of these fitted lines gives parametrized formulae

$$\Delta\tau_1 = 0.32\sqrt{\frac{\Delta K}{U_p}}, \tag{16}$$

and

$$\Delta\tau_2 = 0.97\sqrt{\frac{\Delta K}{U_p}}, \tag{17}$$

where $\Delta\tau_1$ and $\Delta\tau_2$ derived respectively from the energy distributions $h_1(t)$ and $h_2(t)$ are the time durations corresponding to a bandwidth ΔK of high energy HHG radiations. Obviously, $\Delta\tau_2$ is three times of $\Delta\tau_1$ for the same bandwidth ΔK.

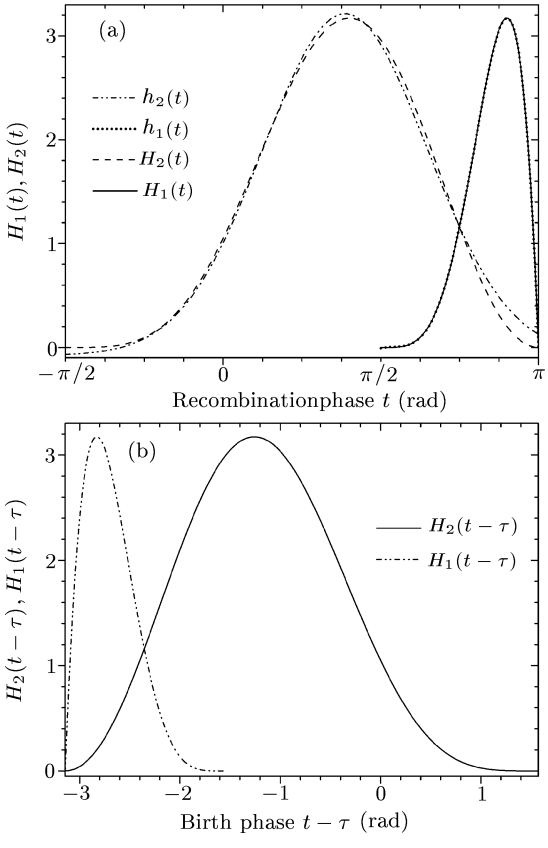


Fig. 3. (a) Harmonic energy distribution $H_1(t)$ and $H_2(t)$ versus the recombination phase t in a laser optical cycle. Here $h_1(t)$ is the Gaussian fit of $H_1(t)$, and $h_2(t)$ is the Polynomial fit of $H_2(t)$. (b) Harmonic energy distribution $H_1(t-\tau)$ and $H_2(t-\tau)$ versus the birth phase $t-\tau$.

For comparison, Fig. 3(b) depicts the harmonic energy distribution $H_1(t-\tau)$ (dot-dot-dashed line) and $H_2(t-\tau)$ (solid line) versus the birth phase $t-\tau$.

In conclusion, the higher energy harmonics can be generated by tunnelling-away electrons in a laser optical cycle. The energy of HHG radiation has two interesting temporal distributions. One is narrow with an asymmetric shape peaked at the laser phase of 161.96°, the other is wide with a symmetric Gaussian shape centred at the laser phase of 71.8°. For the radiations near cut-off edge, Eqs. (16) and (17) depict the relations between a specified time duration of the HHG radiation and the bandwidths of energy distributions. These results may be useful to study, to separate and to apply attosecond x-ray pulses. By applying transfer equations in high time resolution experiments, this two-peak structure of the harmonic energy distributions may be characterized.

It is interesting to produce and apply standard attosecond pulses in experiments. Such pulses are important for applications of attosecond metrology and ultrashort light sources. With pulses of definite phase interval in a laser optical cycle, the ultra-fast measuring system can be calibrated, and the results can be evaluated. Moreover, with parameters precisely measured x-rays as pump and probe pulses, the ultra-fast dynamic processes of chemical or bio-chemical reactions may be simulated and studied in real time.

The author thanks Professor M. Lewenstein for discussion at the Institut de Ciencies Fotoniques, B. S. Zhao at Xi'an Institute of Optics and Precision Mechanics, Chinese Academy of Sciences, Z. Y. Wei at the Institute of Physics, Chinese Academy of Sciences, Y. L. Ye, D. X. Jiang, S. Q. Liu and H. T. Liu at Peking University.

References

[1] Lewenstein M et al 1994 *Phys. Rev.* A **49** 2117
[2] Spielmann Ch and Burnett N B 1997 *Science* **278** 661
[3] Schnurer M et al 1998 *Phys. Rev. Lett.* **80** 3236
[4] Drescher M et al 2001 *Science* **291** 1923
[5] Hentschel M et al 2001 *Nature* **414** 509
[6] Drescher M et al 2002 *Nature* **419** 803
[7] Ge Y C 2005 *Chin. Phys. Lett.* **22** 349
[8] Ge Y C 2005 *Chin. Phys. Lett.* **22** 1916
[9] Ge Y C 2006 *Chin. Phys. Lett.* **23** 143
[10] Yang L Z et al 2004 *Chin. Phys. Lett.* **21** 1259
[11] Zhu C J et al 2005 *Chin. Phys. Lett.* **22** 611